

Lifshitz transitions via the type-II Dirac and type-II Weyl points

G.E. Volovik^{1,2}

¹*Low Temperature Laboratory, Aalto University, P.O. Box 15100, FI-00076 Aalto, Finland*

²*Landau Institute for Theoretical Physics, acad. Semyonov av., 1a, 142432, Chernogolovka, Russia*

(Dated: December 9, 2024)

The type-II Weyl and type-II Dirac points may emerge in relativistic systems. In particular, they may emerge behind the event horizon of black holes. At the Lifshitz transition between type-I and type-II fermions the Dirac lines may emerge, which are supported by the combined action of topology and symmetry. Example is provided by the chiral superfluid, which flows with respect to the heat bath: the Dirac lines appear, when the flow velocity reaches the characteristic "speed of light". The type-II Weyl and Dirac points may also emerge as the intermediate states of the topological Lifshitz transition, at which Fermi surfaces exchange their topological charges. This is illustrated in particular for the relativistic system.

PACS numbers:

I. INTRODUCTION

Weyl fermions¹ are the building blocks of Standard Model. The elementary particles of Standard Model are Weyl fermions with a very pronounced asymmetry between the $SU(2)$ doublet of left-handed Weyl fermions and the $SU(2)$ singlet of right-handed Weyl fermions. The Dirac particles below the electroweak transition are the composite objects obtained by the doublet-singlet mixing of Weyl fermions. In condensed matter the Weyl fermionic excitations live in the vicinity of the topologically protected touching point of two bands.^{2,3} Such diabolical point can be considered as the monopole in the Berry phase flux,^{4,5} and it is described by the momentum-space topological invariant, Chern number, $N_3 = \pm 1$.⁵ The Dirac point has $N_3 = 0$. The Weyl point with higher Chern numbers, $|N_3| > 1$, describes the higher order touching of bands.⁶

Weyl fermions are known to exist in superfluid $^3\text{He-A}$, where the related effects – chiral anomaly^{5,7} and chiral magnetic effect^{8,9} – have been experimentally observed, and in electronic topological semimetals.^{10–20} Recently the attention is attracted to the so-called type-II Weyl points.^{21–27} In relativistic theories such points emerge either behind the event horizon,^{5,28} or as the intermediate states of the topological quantum phase transition.^{29,30} We consider here both cases.

II. DIRAC LINE AT THE TRANSITION BETWEEN TYPE I AND TYPE-II WEYL POINTS

The type-II Weyl fermions may appear in relativistic theories, if the relativistic Weyl fermions are not fundamental and emerge in the low energy sector of the fermionic quantum vacuum. In particular, they may emerge, for example, in the vacuum of the real (Majorana) fermions.³¹ Then the Hamiltonian describing the Weyl fermions in the vicinity of the topologically protected Weyl point at $\mathbf{p}^{(0)}$ has the general form

$$H = e_k^j(p_j - p_j^{(0)})\hat{\sigma}^k + e_0^j(p_j - p_j^{(0)}). \quad (1)$$

This expansion suggests that position $\mathbf{p}^{(0)}$ of the Weyl point gives rise to the effective $U(1)$ gauge field, while e_k^j and e_0^j play the role of the emergent tetrad fields. The energy spectrum of the Weyl fermions depends on the ratio between the two terms in the rhs of Eq.(1), i.e. on the parameter $|e_0^j[e^{-1}]_j^k|$.³¹ When $|e_0^j[e^{-1}]_j^k| < 1$ one has the conventional Weyl point, while at $|e_0^j[e^{-1}]_j^k| > 1$ this Weyl point transforms to two Fermi surfaces, which touch each other. This regime is now called the type-II Weyl.²¹

At the transition between the two regimes, at $|e_0^j[e^{-1}]_j^k| = 1$, one has the Fermi (Dirac) line. This nodal line is protected by topology (in combination with symmetry). Let us consider the corresponding topological charge of the nodal line using a simple choice for the tetrad field, with $e_k^j = c\delta_k^j$ and $e_0^j = -fc\hat{z}^j$ where f is parameter:

$$H = c\boldsymbol{\sigma} \cdot \hat{\mathbf{p}} - fcp_z. \quad (2)$$

For $f \neq 0$ the Weyl cone is tilted, and for $f > 1$ the type-II Weyl point takes place. At the boundary between the two regimes, at $f = 1$, there is the Dirac line on the p_z -axis, i.e. at $p_\perp = 0$. The topological invariant describing this

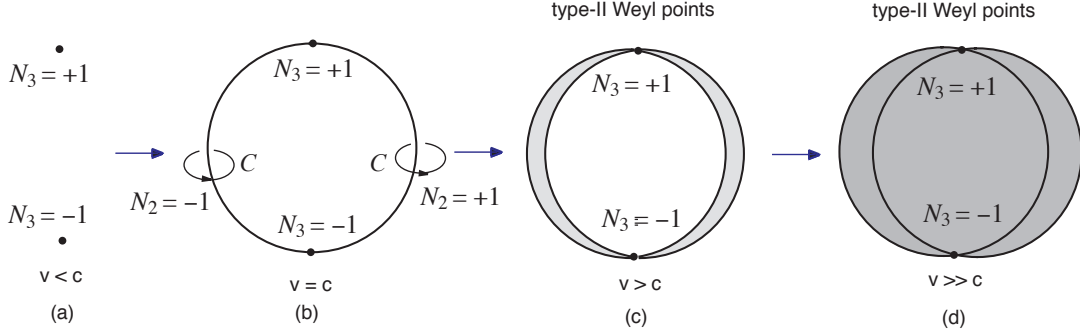


FIG. 1: Formation of type-II Weyl points when the flow velocity v exceeds the pair-breaking velocity c . (a): Two Weyl points in spectrum of ${}^3\text{He-A}$ at $v < c$. (b): At critical velocity $v = c$ the Dirac lines appear which connect the Weyl points. (c): At $v > c$ the type-II Weyl points are formed. (d): at large $v \gg c$ the Fermi surfaces overlap.

line is

$$N_2 = \mathbf{tr} \oint_C \frac{dl}{4\pi i} \cdot [\sigma_z H_{f=1}^{-1}(\mathbf{p}) \partial_l H_{f=1}(\mathbf{p})], \quad (3)$$

where C is the contour in momentum space around the p_z -axis. This integral is integer, $N_2 = 1$, only for $f = 1$, when the Hamiltonian anticommutes with σ_z . For $f \neq 1$ the symmetry of the Hamiltonian is lost, the integral depends on p_z and on the radius of the contour C . Only for $p_z = 0$ the integral remains integer for any f . The Dirac line emerges for the relativistic fermions and disappears, when the higher order nonrelativistic corrections are taken into account and the symmetry responsible for the stability of the Dirac line is lost.

The Dirac lines exist at the transition between the type-I and type-II Weyl fermions in the chiral superfluid, such as superfluid ${}^3\text{He-A}$. The simple model Hamiltonian for chiral superfluid is⁵

$$H = p_x v + \tau_3 \frac{p^2 - p_F^2}{2m} + \tau_1 c p_x + \tau_2 c p_y, \quad (4)$$

with $\mathbf{v} = v\hat{\mathbf{x}}$ being the superfluid velocity with respect to the heat bath. The first term in the rhs of Eq. (4) is the Doppler shift; τ_i are the Pauli matrices in the Bogoliubov-Nambu space; in ${}^3\text{He-A}$ $v_F = p_F/m \gg c$. The transition between the type-I Weyl fermions and the type-II Weyl fermions takes place, when the flow velocity v reaches the "speed of light" c , see Fig. 1. For $v < c$ there are two Weyl points at $\mathbf{p}^{(0)} = \pm p_F \hat{\mathbf{z}}$ with opposite topological charges $N_3 = \pm 1$. At $v > c$ there are two banana shape Fermi surfaces, which contact each other at the type-II Weyl points, see Fig. 1(c). Finally at $v_F > v \gg c$ these Fermi surfaces overlap and form two Fermi surfaces, which cross each other at the type-II Weyl points in Fig. 1(d). Exactly at the Lifshitz transition, at $v = c$, one has Dirac lines, which connect the Weyl points in Fig. 1(b). These lines are described by the invariant N_2 in Eq.(3), where the symmetry operator is τ_1 instead of σ_z .

III. TYPE II WEYL FERMIONS BEHIND THE BLACK HOLE HORIZON

The transition between the type I and type-II Weyl points may occur for the relativistic fermions at the horizon of the black hole.

In general relativity the stationary metric for the black hole both outside and inside the horizon is provided in the Painlevé-Gullstrand spacetime.³² The line element of the Painlevé-Gullstrand metric is equivalent to the so-called acoustic metric:^{33,34}

$$ds^2 = -c^2 dt^2 + (d\mathbf{r} - \mathbf{v} dt)^2 = -(c^2 - v^2) dt^2 - 2\mathbf{v} d\mathbf{r} dt + d\mathbf{r}^2. \quad (5)$$

This is stationary but not static metric, which is expressed in terms of the velocity field $\mathbf{v}(\mathbf{r})$ describing the drag in the gravitational field. For the spherical black hole the velocity field is radial:

$$\mathbf{v}(\mathbf{r}) = -\hat{\mathbf{r}} c \sqrt{\frac{r_h}{r}}, \quad r_h = \frac{2MG}{c^2}. \quad (6)$$

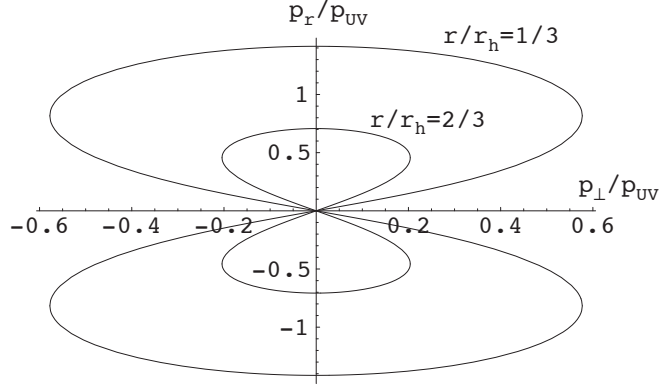


FIG. 2: Fermi surfaces of the type-II Weyl fermions in Standard Model behind the black hole horizon (from Ref.²⁸). Here p_r is the radial component of the momentum \mathbf{p} ; $p_\perp = \sqrt{p^2 - p_r^2}$; and $p_{UV} = E_{UV}/c$ is the ultraviolet cut-off at which the Lorentz invariance is violated.

Here M is the mass of the black hole; r_h is the radius of the horizon; G is the Newton gravitational constant. The minus sign in Eq.(6) gives the metric for the black hole, while the plus sign would characterize the white hole. The corresponding tetrad fields are $e_k^j = c\delta_k^j$ and $e_0^j = v^j$.³⁵

We are interested in the spectrum behind the black hole horizon, where the drag velocity exceeds the speed of light, $\mathbf{v}^2(\mathbf{r}) > c^2$. Near the horizon of the black hole and inside the horizon the particle masses can be neglected, and one can consider the left handed and right handed fermions independently. Near the horizon the Dirac cone is tilted, and behind the horizon it crosses zero energy and forms the Fermi surfaces corresponding to the type-II Weyl points. The Hamiltonian for the fundamental Weyl fermions in the Painlevé-Gullstrand metric has the form:²⁸

$$H = \pm c\boldsymbol{\sigma} \cdot \mathbf{p} - p_r v(r) + \frac{c^2 p^2}{E_{UV}}, \quad v(r) = c\sqrt{\frac{r_h}{r}}. \quad (7)$$

Here the plus and minus signs correspond to the right handed and left handed fermions respectively; p_r is the radial momentum of fermions. The second term in the rhs of (7) is the Doppler shift due to the drag velocity, $\mathbf{p} \cdot \mathbf{v}(\mathbf{r})$ (compare with Eq.(4) for chiral superfluid). The third term is the added nonlinear dispersion. The latter is natural for the condensed matter systems. The parameter E_{UV} is the ultraviolet (UV) energy scale at which the violation of the Lorentz invariance is expected. Most probable is that this UV scale is much higher than the Planck energy scale. In principle, such term can arise in effective Hamiltonian $H = G^{-1}(\omega = 0, \mathbf{p})$ even without violation of Lorentz invariance on fundamental level:³⁶ the Green's function $G(\omega, \mathbf{p})$ may still be relativistic invariant, while the Lorentz invariance of the Hamiltonian is violated due to the existence of the heat bath reference frame. The p^2 term makes the Fermi surfaces attached to the Weyl II point closed. The p^2 term can be considered as a small correction only when $cp \ll E_{UV}$. As we shall see, this is valid if the spectrum inside the black hole is considered near the horizon, where $r_h - r \ll r_h$.

Behind the black hole horizon, i.e. at $r < r_h$, the Weyl point in the spectrum transforms to the pair of the closed Fermi surfaces with the touching point: the type-II Weyl point. The Fermi surfaces are shown in Fig. 2 at two positions inside the black hole: at $r = r_h/3$ and $r = 2r_h/3$. Close to the horizon the Fermi surfaces are concentrated in the region $|p_r| < p_{UV}(v(r) - c)/c \ll p_{UV}$.

IV. LIFSHITZ TRANSITIONS WITH TYPE-II WEYL AND DIRAC POINTS AT THE TRANSITION

The type-II Weyl point demonstrates the interplay of different topological invariants. There are: (i) the invariant N_1 , which is responsible for the local stability of the Fermi surface;⁵ (ii) the invariant N_3 , which is the global invariant describing the whole system: when the Fermi surfaces collapse to a point, this is the topological charge of the Weyl point; (iii) in addition, the touching point of two Fermi surfaces can be characterized by the N_2 topological invariant in Eq.(3), if C is chosen as an infinitesimal contour in momentum space around the touching point, see also Ref.²².

The interplay of the invariants leads to the various Lifshits transitions accompanied by the change of the topology: topological quantum phase transitions. Some of them are shown in Figures 3, 4 and 5.

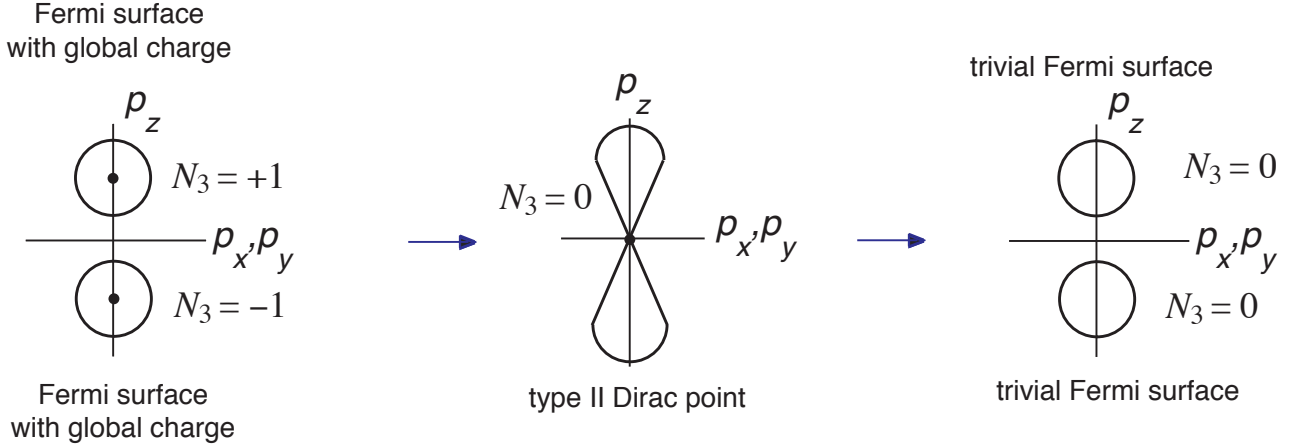


FIG. 3: Illustration of the process of the transfer of the Chern number N_3 between the Fermi surfaces as topological Lifshitz transition. Relativistic Weyl fermions in Eq.(8) are considered.^{29,30} (left): Fermi surfaces of the right and left Weyl fermions. They enclose the Weyl points with topological charge $N_3 = +1$ and $N_3 = -1$ respectively. (right): Fermi surfaces are topologically trivial. (middle): At the border between the two regimes the Fermi surfaces touch each other and transfer the topological charge. This intermediate state represents the type-II Dirac point with topological charge $N_3 = 0$.

Fig. 3 demonstrates the Lifshitz transition, where the intermediate state represents the type-II Dirac point. Such transition has been discussed in relativistic theory with the CPT-violating perturbation.^{29,30} The corresponding Hamiltonian for a massive Dirac particle with mass M has the form:

$$H = \begin{pmatrix} \boldsymbol{\sigma} \cdot (c\mathbf{p} - \mathbf{b}) - b_0 & M \\ M & -\boldsymbol{\sigma} \cdot (c\mathbf{p} + \mathbf{b}) + b_0 \end{pmatrix}. \quad (8)$$

Here the 4-vector $b_\mu = (b_0, \mathbf{b})$ causes the shift of the Weyl points in opposite direction and formation of two Fermi surfaces at $\mathbf{b}^2 > b_0^2 + M^2$. One Fermi surface is formed by the right-handed Weyl fermions; it encloses the Weyl point with nonzero topological charge $N_3 = +1$. The other one is the Fermi surface of the left-handed Weyl fermions; it encloses the Weyl point with nonzero topological charge $N_3 = -1$. At $M^2 < \mathbf{b}^2 < b_0^2 + M^2$ the global topology of the Fermi surfaces becomes trivial, with $N_3 = 0$ for each of them. The quantum phase transition between the Fermi surfaces with nonzero and trivial topological charge N_3 occurs at $\mathbf{b}^2 = b_0^2 + M^2$. At this transition, the Fermi surfaces touch each other, and their topological charges annihilate each other. The intermediate state, at which the Fermi surfaces touch each other, is the type-II Dirac point. As distinct from the type-II Weyl point, the topological charge of the type-II Dirac point is $N_3 = 0$.

Fig. 4 and Fig. 5 demonstrate the Lifshitz transitions, at which the intermediate state represents the type-II Weyl point with topological charge $N_3 = 1$. In Fig. 4 the Fermi surface with the global topological charge $N_3 = 1$ and the topologically trivial Fermi surface with $N_3 = 0$ exchange their topological charges. In Fig. 5 two Fermi surfaces loose at Lifshitz transition the Weyl point with topological charge $N_3 = 1$ (see details in Ref.³⁷). The latter can be illustrated by the Hamiltonian

$$H = c\boldsymbol{\sigma} \cdot (\mathbf{p} - \mathbf{p}^{(0)}) + \frac{p^2 - p_F^2}{2m}, \quad (9)$$

for $p_F > mc$. The Lifshitz transition occurs at $|\mathbf{p}^{(0)}| = p_F$.

For comparison consider the type-II Weyl points in superfluid $^3\text{He-A}$ in supercritical regime in Fig. 1(d), when the flow velocity v exceeds the pair breaking velocity c .

V. CONCLUSION

The interplay of different topological invariants enhances the variety of the topological Lifshitz transitions. Here we discussed the examples of the transition, which involves the Fermi surfaces with topological charge N_1 , Weyl points with the topological charge N_3 and Dirac lines with topological charge N_2 . Depending on the type of the transition,

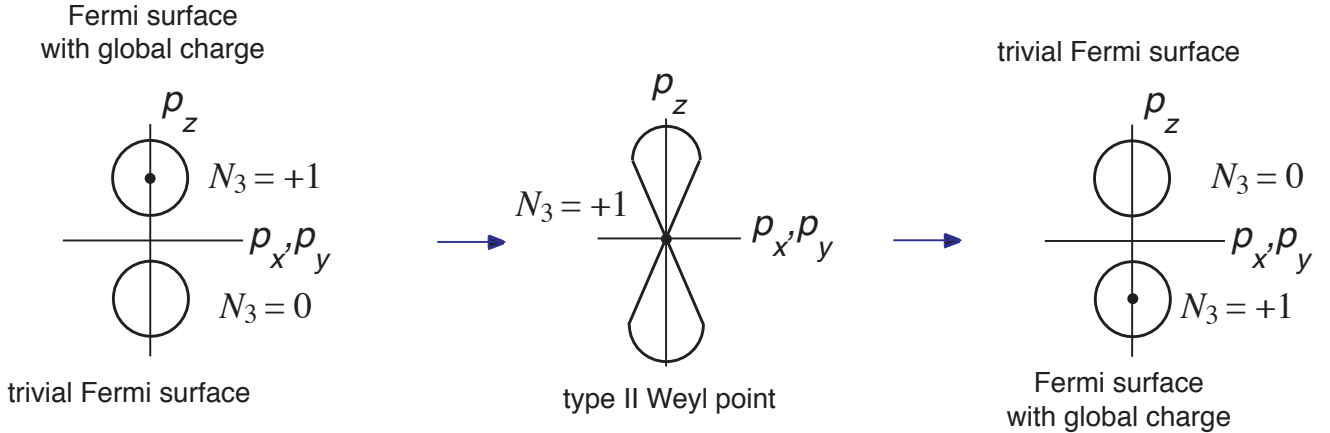


FIG. 4: Illustration of the process of the topological charge transfer between the Fermi surfaces through the type-II Weyl point. *left*: The upper Fermi surface has non-zero global charge. It encloses the Weyl point with $N_3 = 1$. The lower Fermi surface is topologically trivial. *right*: The upper Fermi surface is trivial, while the lower one has the global topological charge $N_3 = 1$. (*middle*): Transfer of the Chern number between topological and non-topological Fermi surfaces occurs via the intermediate state, at which the Fermi surfaces touch each other. The touching point is the type-II Weyl point with topological charge $N_3 = +1$.

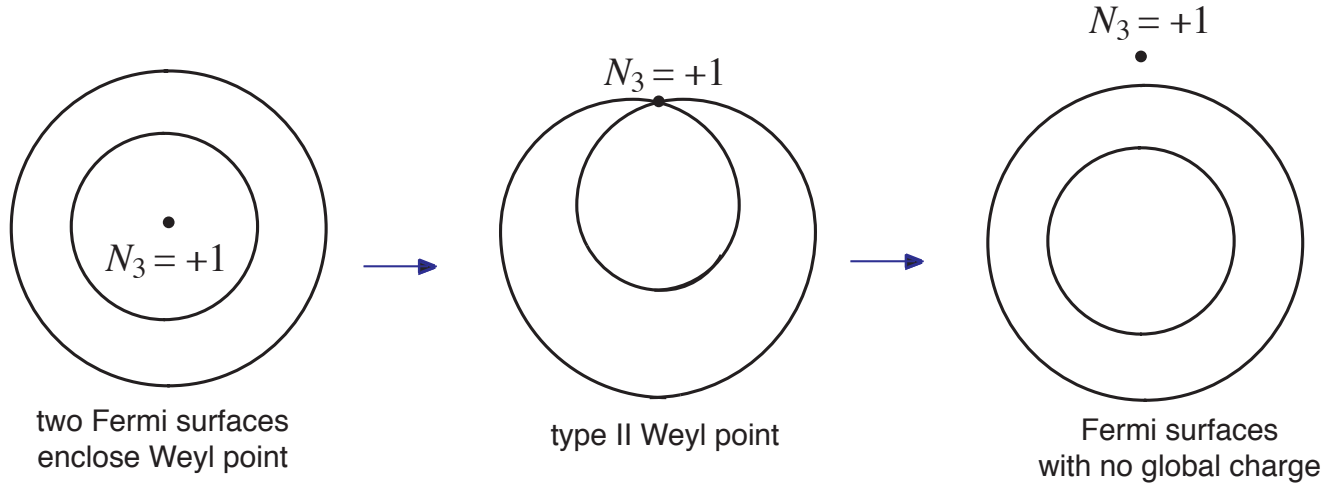


FIG. 5: Illustration of the process of the topological charge transfer. (*left*): Both inner and outer Fermi surfaces enclose the Weyl point with topological charge $N_3 = +1$. (*right*): Both inner and outer Fermi surfaces have trivial topological charge $N_3 = 0$. (*middle*): The intermediate state, at which the Fermi surfaces touch each other, is the type-II Weyl point with topological charge $N_3 = +1$.

the intermediate state has the type-II Dirac point, the type-II Weyl point or the Dirac line supported by symmetry and topology. Many other Lifshitz transitions are expected, since we did not touch here the other possible topological features: topological invariants which describe the shape of the Fermi surface; the shape of the Dirac nodal lines; their interconnections; etc. The interplay of topologies can be seen in particular in the electronic spectrum of Bernal and rombohedral graphite.³⁸⁻⁴¹

I thank Ivo Souza for pointing out mistake in the early version.

¹ H. Weyl, Elektron und gravitation, I. Z. Phys. **56**, 330–352 (1929).

² J. von Neumann and E. Wigner, Über das Verhalten von Eigenwerten bei adiabatischen Prozessen, Phys. Z. **30**, 467 (1929).

³ S.P. Novikov, Magnetic Bloch functions and vector bundles. Typical dispersion laws and their quantum numbers, Sov. Math., Dokl. **23**, 298–303 (1981).

⁴ G.E. Volovik, Zeros in the fermion spectrum in superfluid systems as diabolical points, JETP Lett. **46**, 98–102 (1987).

⁵ G.E. Volovik, *The Universe in a Helium Droplet*, Clarendon Press, Oxford (2003).

⁶ G.E. Volovik, V.A. Konyshov, Properties of the superfluid systems with multiple zeros in fermion spectrum, JETP Lett. **47**, 250–254 (1988).

⁷ T.D.C. Bevan, A.J. Manninen, J.B. Cook, J.R. Hook, H.E. Hall, T. Vachaspati and G.E. Volovik, Momentum creation by vortices in superfluid ^3He as a model of primordial baryogenesis, Nature **386**, 689–692 (1997).

⁸ M. Krusius, T. Vachaspati and G.E. Volovik, Flow instability in ^3He -A as analog of generation of hypermagnetic field in early Universe, cond-mat/9802005.

⁹ G.E. Volovik, Axial anomaly in ^3He -A: Simulation of baryogenesis and generation of primordial magnetic field in Manchester and Helsinki, Physica B **255**, 86–107 (1998); cond-mat/9802091.

¹⁰ C. Herring, Accidental degeneracy in the energy bands of crystals, Phys. Rev. **52**, 365–373 (1937).

¹¹ A.A. Abrikosov and S.D. Beneslavskii, Possible existence of substances intermediate between metals and dielectrics, JETP **32**, 699–798 (1971).

¹² A.A. Abrikosov, Some properties of gapless semiconductors of the second kind, J. Low Temp. Phys. **5**, 141–154 (1972).

¹³ H.B. Nielsen and M. Ninomiya, The Adler-Bell-Jackiw anomaly and Weyl fermions in a crystal, Phys. Lett. B **130**, 389–396 (1983).

¹⁴ A.A. Burkov and L. Balents, Weyl semimetal in a topological insulator multilayer, Phys. Rev. Lett. **107**, 127205 (2011).

¹⁵ A.A. Burkov, M.D. Hook, L. Balents, Topological nodal semimetals, Phys. Rev. B **84**, 235126 (2011).

¹⁶ Hongming Weng, Chen Fang, Zhong Fang, B. Andrei Bernevig, Xi Dai, Weyl semimetal phase in noncentrosymmetric transition-metal monophosphides, Phys. Rev. X **5**, 011029 (2015).

¹⁷ Shin-Ming Huang, Su-Yang Xu, Ilya Belopolski, Chi-Cheng Lee, Guoqing Chang, BaoKai Wang, Nasser Alidoust, Guang Bian, Madhab Neupane, Chenglong Zhang, Shuang Jia, Arun Bansil, Hsin Lin and M. Zahid Hasan, A Weyl fermion semimetal with surface Fermi arcs in the transition metal monopnictide TaAs class, Nat. Commun. **6**, 7373 (2015).

¹⁸ B.Q. Lv, H.M. Weng, B.B. Fu, X.P. Wang, H. Miao, J. Ma, P. Richard, X.C. Huang, L.X. Zhao, G.F. Chen, Z. Fang, X. Dai, T. Qian, and H. Ding, Experimental discovery of Weyl semimetal TaAs, Phys. Rev. X **5**, 031013 (2015).

¹⁹ Su-Yang Xu, I. Belopolski, N. Alidoust, M. Neupane, Guang Bian, Chenglong Zhang, R. Sankar, Guoqing Chang, Zhujun Yuan, Chi-Cheng Lee, Shin-Ming Huang, Hao Zheng, Jie Ma, D.S. Sanchez, BaoKai Wang, A. Bansil, Fangcheng Chou, P.P. Shibayev, Hsin Lin, Shuang Jia, M. Zahid Hasan, Discovery of a Weyl fermion semimetal and topological Fermi arcs, Science **349**, 613–617 (2015).

²⁰ Ling Lu, Zhiyu Wang, Dexin Ye, Lixin Ran, Liang Fu, John D. Joannopoulos, Marin Soljacic, Experimental observation of Weyl points, Science **349**, 622–624 (2015).

²¹ Alexey A. Soluyanov, Dominik Gresch, Zhijun Wang, QuanSheng Wu, Matthias Troyer, Xi Dai, B. Andrei Bernevig, Type-II Weyl semimetals, Nature **527**, 495–498 (2015).

²² Yong Xu, Fan Zhang, and Chuanwei Zhang, Structured Weyl points in spin-orbit coupled fermionic superfluids, Phys. Rev. Lett. **115**, 265304 (2015).

²³ Tay-Rong Chang, Su-Yang Xu, Guoqing Chang, Chi-Cheng Lee, Shin-Ming Huang, BaoKai Wang, Guang Bian, Hao Zheng, Daniel S. Sanchez, Ilya Belopolski, Nasser Alidoust, Madhab Neupane, Arun Bansil, Horng-Tay Jeng, Hsin Lin, and M. Zahid Hasan, Prediction of an arc-tunable Weyl Fermion metallic state in $\text{Mo}_x\text{W}_{1-x}\text{Te}_2$, Nature Com. **7**, 10639 (2016).

²⁴ G. Autes, D. Gresch, A. A. Soluyanov, M. Troyer and O.V. Yazyev, Robust type-II Weyl semimetal phase in transition metal diphosphides XP_2 ($\text{X} = \text{Mo, W}$), arXiv:1603.04624.

²⁵ Su-Yang Xu, Nasser Alidoust, Guoqing Chang, Hong Lu, Bahadur Singh, Ilya Belopolski, Daniel S. Sanchez, Xiao Zhang, Guang Bian, Hao Zheng, Marius-Adrian Husanu, Yi Bian, Shin-Ming Huang, Chuang-Han Hsu, Tay-Rong Chang, Horng-Tay Jeng, Arun Bansil, Vladimir N. Strocov, Hsin Lin, Shuang Jia, and M. Zahid Hasan, Discovery (theoretical and experimental) of Lorentz-violating Weyl fermion semimetal state in LaAlGe materials, arXiv:1603.07318.

²⁶ J. Jiang, Z. K. Liu, Y. Sun, H. F. Yang, R. Rajamathi, Y.P. Qi, L.X. Yang, C. Chen, H. Peng, C.-C. Hwang, S. Z. Sun, S.-K. Mo, I. Vobornik, J. Fujii, S.S.P. Parkin, C. Felser, B.H. Yan, and Y. L. Chen, Observation of the type-II Weyl semimetal phase in MoTe_2 , arXiv:1604.00139.

²⁷ T.E. O'Brien, M. Diez, C.W.J. Beenakker, Magnetic breakdown and Klein tunneling in a type-II Weyl semimetal, arXiv:1604.01028.

²⁸ P. Huhtala and G.E. Volovik, Fermionic microstates within Painlevé-Gullstrand black hole, ZhETF **121**, 995–1003; JETP **94**, 853–861 (2002); gr-qc/0111055.

²⁹ F.R. Klinkhamer and G.E. Volovik, Emergent CPT violation from the splitting of Fermi points, Int. J. Mod. Phys. A **20**, 2795–2812 (2005); hep-th/0403037.

³⁰ G.E. Volovik, Quantum phase transitions from topology in momentum space, in: "Quantum Analogues: From Phase

Transitions to Black Holes and Cosmology”, eds. William G. Unruh and Ralf Schützhold, Springer Lecture Notes in Physics **718**, 31–73 (2007).

³¹ G.E. Volovik and M.A. Zubkov, Emergent Weyl spinors in multi-fermion systems, Nuclear Physics B **881**, 514 (2014).

³² P. Painlevé, La mécanique classique et la théorie de la relativité, C. R. Hebd. Acad. Sci. (Paris) **173**, 677-680 (1921); A. Gullstrand, Allgemeine Lösung des statischen Einkörperproblems in der Einsteinschen Gravitationstheorie, Arkiv. Mat. Astron. Fys. **16**, 1-15 (1922).

³³ W. G. Unruh, Experimental black-hole evaporation? Phys. Rev. Lett. **46**, 1351-1354 (1981); Sonic analogue of black holes and the effects of high frequencies on black hole evaporation, Phys. Rev. D **51**, 2827-2838 (1995).

³⁴ Per Kraus and Frank Wilczek, Some applications of a simple stationary line element for the Schwarzschild geometry, Mod. Phys. Lett. A **9**, 3713–3719 (1994).

³⁵ C. Doran, New form of the Kerr solution, Phys. Rev. D **61**, 067503 (2000).

³⁶ G.E. Volovik, Topological invariants for Standard Model: from semi-metal to topological insulator, JETP Lett. **91**, 55–61 (2010); arXiv:0912.0502.

³⁷ D. Gosalbez-Martinez, I. Souza, D. Vanderbilt, Chiral degeneracies and Fermi-surface Chern numbers in bcc Fe, Phys. Rev. B **92**, 085138 (2015); arXiv:1505.07727

³⁸ J.W. McClure, Band structure of graphite and de Haas-van Alphen effect, Phys. Rev. **108**, 612-618 (1957).

³⁹ G.P. Mikitik and Yu.V. Sharlai, Band-contact lines in the electron energy spectrum of graphite, Phys. Rev. B **73**, 235112 (2006).

⁴⁰ G.P. Mikitik and Yu.V. Sharlai, The Berry phase in graphene and graphite multilayers, Low Temp. Phys. **34**, 794–780 (2008).

⁴¹ T.T. Heikkilä and G.E. Volovik, Nexus and Dirac lines in topological materials, New J. Phys. **17**, 093019 (2015).